

Reinforcement Learning Trajectory Generation and Control for Aggressive Perching on Vertical Walls with Quadrotors

Chen-Huan Pi, Kai-Chun Hu, Yu-Ting Huang, Stone Cheng

Abstract—Micro aerial vehicles are widely being researched and employed due to their relative low operation costs and high flexibility in various applications. We study the under-actuated quadrotor perching problem, designing a trajectory planner and controller which generates feasible trajectories and drives quadrotors to desired state in state space. This paper proposes a trajectory generating and tracking method for quadrotor perching that takes the advantages of reinforcement learning controller and traditional controller. The trained low-level reinforcement learning controller would manipulate quadrotor toward the perching point in simulation environment. Once the simulated quadrotor has successfully perched, the relative trajectory information in simulation will be sent to tracking controller on real quadrotor and start the actual perching task. Generating feasible trajectories via the trained reinforcement learning controller requires less time, and the traditional trajectory tracking controller could easily be modified to control the quadrotor and mathematically analysis its stability and robustness. We show that this approach permits the control structure of trajectories and controllers enabling such aggressive maneuvers perching on vertical surfaces with high precision.

Index Terms—Aggressive flight, reinforcement learning, quadrotor

I. INTRODUCTION

Micro Aircraft Vehicles (MAVs) are widely being researched and employed due to their relative low operation costs and high flexibility in various applications. The applications include search and rescue [2], wind turbine inspection [13], [8], reconnaissance and mapping [3], target tracking, environmental monitoring, etc.

Most of the quadrotor is powered by battery for motor driving and generate lift, which gives a limited time for quadrotor tasks performing. Flying with a power cable connected to power supply on ground [5], [1], [9] can solve the problem but the quadrotor can only be operated in a specific and relative open area. If the quadrotor can perch on arbitrary angle surface such as vertical wall to reduce its battery consumption while keeping environment monitoring using on-board camera or even for battery charging. The mission time can be extended with a great amount of time.

The quadrotor is an under-actuated system, meaning it cannot control its position while maintaining arbitrary attitude. To successfully perch on the wall, quadrotors using gripper mechanism [16], [18], [7] to perch on vertical walls had been proposed. However, the perching device would cost additional energy consumption. Another approach for perching is using aggressive maneuver to land without adding mechanism on quadrotor.

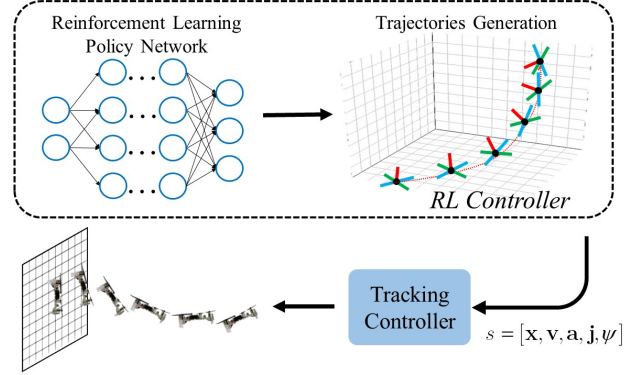


Fig. 1: Aggressive perching maneuver using reinforcement learning trajectory planner and tracking controller

There are a few other researches discussing perching of traditional quadrotors. To land a traditional quadrotor, the process can be separated into two different parts, 1) Trajectory planning to the target landing point. 2) Track the designed trajectory and land. To generate a feasible trajectory, Quadratic Program problem were formulated under the dynamics constrain of quadrotor [17], [11].

Using Reinforcement Learning (RL) for low-level quadrotor control has been proposed and shown its implementation result in real world quadrotor to stabilize and hover or fly on a specific trajectory [6], [12]. The advantage of using RL controller is due to its nonlinearity and fast computation. However, there exist a gap showing on the tracking result while transferring the RL controller on quadrotors from simulation to real world experiment. In reality condition, the quadrotor hovering and tracking results didn't perform as same as the results in simulation. The reason is that the RL-based controller is sensitive to the deviation of model physical parameters such as take-off weight or motor characteristic. This situation can be harsher when considering aggressive maneuver using RL controlling the motors directly.

To fix this problem, we propose a method that takes the advantages of RL controller and traditional controller illustrated in Fig. 1. First, we train a RL controller to learn how to perch the quadrotor to the set point by directly command the thrust force of each motor. Second, we create a simulated quadrotor which has the same initial states as the real quadrotor. The trained low-level RL controller would manipulate quadrotor toward the landing point in simulation environment. Third,

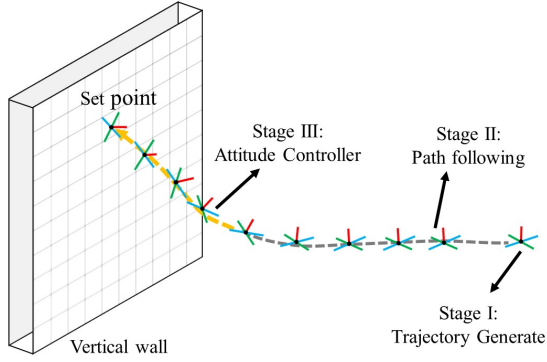


Fig. 2: The quadrotor launch in random initial state. Stage I generate the trajectory of perching. In Stage II, the quadrotor start to track along the planned trajectory and switch to Stage III for attitude control while it approach to landing position.

we extract the trajectory information in simulation and send it to traditional controller on real quadrotor. Generating feasible trajectories via the trained RL controller would require less time, and the traditional trajectory tracking controller could easily be modified to control the quadrotor and mathematically analysis its stability and robustness. Moreover, this combined structure of controller can be implement to different physical parameters or different type of vehicle.

In Section II, the dynamics of quadrotor and reinforcement learning algorithm were presented. Section III and Section IV describes the RL perching training for trajectory generating and the traditional controller design to perform perching task. Section V shows the successful application of the combined structure to the quadrotor, and Section VI conclude the paper.

II. METHODOLOGY

The first challenge of planning is that since the quadrotor is an under-actuated system, the designed trajectory needs to be feasible with respect to the system dynamic constrains. A possible technique is to solve a constrained optimization, for example:

$$\begin{aligned} \min_a \int_{t_i}^{t_f} R(x, \dot{x}, a) dt + T(x(t_f)) \\ \dot{x} = f(x, a) \\ x(t_i) = x_0 \end{aligned} \quad (1)$$

where R is run time cost, T terminal cost, f system dynamic, a input action, and x_0 is the initial state. With this scheme, we can obtain a suitable trajectory $x(t)$ with respect to time.

In this paper, we assuming dynamic trajectory planning problem can be described by a Markov decision processes (MDP), with this property the best decisions are independent to the history. Next, we utilize reinforcement learning to search the feasible solutions in (1) while the searching results were memorized by an artificial neural network. With this scheme, the searching cost passes through the training phase.

A. Reinforcement Learning

Reinforcement learning (RL) is one of basic machine learning paradigms, aim to solve MDP through learning processes. In this section, we provide a short introduction to reinforcement learning.

A Markov decision processes is described by a 4-tuple $(\mathcal{S}, \mathcal{A}, \mathcal{P}, r)$ where \mathcal{S} is the state space, \mathcal{A} is action space, $\mathcal{P} = \mathcal{P}(s_{t+1}|s_t = s \in \mathcal{S}, a_t = a \in \mathcal{A})$ is transition probability and $r = r(s, a) \in \mathbb{R}$ is the reward function. The goal of MDPs is to find a policy

$$\pi = \pi(a \in \mathcal{A}|s) \quad (2)$$

that maximize cumulative discounted reward

$$\sum_{t=0}^{\infty} \gamma^t r(s_t, a_t), \quad (3)$$

where $\gamma \in (0, 1)$ is discounting factor. To connect (1), we write MDP statement as follow:

$$\begin{aligned} \max_{\pi} \mathbb{E} \left[\sum_{t=0}^{\infty} \gamma^t r_t \mid a_t \sim \pi(a|s_t) \right] \\ s_{t+1} \sim P(s|s_t, a_t) \\ s_0 \sim P_0(s) \end{aligned} \quad (4)$$

where $r_t = r(s_t, a_t)$, P_0 is the initial state distribution. For a given policy π , the following recurrent relation hold

$$V^{\pi}(s_t) = \mathbb{E} \left[r_t + \gamma V^{\pi}(s_{t+1}) \mid a_t \sim \pi(a|s_t) \right], \quad (5)$$

where

$$V^{\pi}(s) = \mathbb{E} \left[\sum_{t=0}^{\infty} \gamma^t r_t \mid a_t \sim \pi(a|s_t), s_0 = s \right]. \quad (6)$$

The quantity

$$A^{\pi}(x, a) = \mathbb{E} [r_t + \gamma V^{\pi}(s_{t+1}) | s_t = x, a_t = a] - V^{\pi}(s) \quad (7)$$

can be used for determine that which action is good with respect to policy π . In fact, we can guarantee [12] that a policy π is better than policy μ if

$$\forall (s, a) \in \mathcal{S} \times \mathcal{A}$$

$$[\pi(a|s) - \mu(a|s)] A^{\mu}(s, a) > 0 \quad (8a)$$

or

$$[\pi(a|s) - \mu(a|s)] A^{\pi}(s, a) > 0. \quad (8b)$$

Therefore, for a policy search iteration, Equation (8) provides an improvement guideline to distinguish whatever an action should be memorized or not.

B. Quadrotor Dynamics

The simplest way to modeling a multi-rotor is considered as a rigid body dynamics

$$\frac{d}{dt} \begin{pmatrix} \mathbf{R} \\ \boldsymbol{\Omega} \\ \mathbf{x} \\ \mathbf{v} \\ \mathbf{a} \end{pmatrix} = \begin{pmatrix} \mathbf{R}\hat{\boldsymbol{\Omega}} \\ \mathbf{J}^{-1}(\boldsymbol{\tau} - \boldsymbol{\Omega} \times \mathbf{J}\boldsymbol{\Omega}) \\ \mathbf{v} \\ \frac{1}{m}\mathbf{R}[0 \ 0 \ T_z]^T + \mathbf{g} \\ \mathbf{s} \end{pmatrix} \quad (9)$$

where \mathbf{R} is rotation matrix, $\boldsymbol{\Omega}$ is angular velocity on body frame, and the *hat map* $\hat{\cdot} : \mathbb{R}^3 \rightarrow SO(3)$ is defined as the condition $\hat{x}y = x \times y, \forall x, y \in \mathbb{R}^3$ [10]. The \mathbf{x} , \mathbf{v} , and \mathbf{a} are position, velocity, acceleration with respect to inertia frame, J is the momentum of inertia, m is the mass of rigid body, \mathbf{g} is the gravity acceleration. The force and moment model of each quadrotor motor can be simplified as

$$F_i = k_F \omega_i^2, M_i = k_M \omega_i^2, \quad (10)$$

where ω_i is the rotation speed of motors and $i = 1, 2, 3, 4$. k_f , k_M are the coefficient of lift and moment. The relation between moment τ , force T_z of quadrotor and motor speed ω_i can be written as

$$\begin{pmatrix} \tau \\ T_z \end{pmatrix} = \begin{pmatrix} \frac{-l}{\sqrt{2}}k_F & \frac{l}{\sqrt{2}}k_F & \frac{l}{\sqrt{2}}k_F & \frac{-l}{\sqrt{2}}k_F \\ \frac{l}{\sqrt{2}}k_F & \frac{-l}{\sqrt{2}}k_F & \frac{l}{\sqrt{2}}k_F & \frac{-l}{\sqrt{2}}k_F \\ k_M & k_M & -k_M & -k_M \\ -1 & -1 & -1 & -1 \end{pmatrix} \begin{pmatrix} \omega_1^2 \\ \omega_2^2 \\ \omega_3^2 \\ \omega_4^2 \end{pmatrix} \quad (11)$$

where l is the physical dimension of quadrotor.

C. Training and Inference

Integrating (9), (11) and Euler method, we can obtain the discrete time transfer function G of a quadrotor

$$s_{t+1} = G(s_t, a_t), \quad (12)$$

where $s_t = (\mathbf{R}, \boldsymbol{\Omega}, \mathbf{x}, \mathbf{v})_t$ and $a_t = (T_1, T_2, T_3, T_4)_t$. We change our objective in terms of deterministic transition and the main objective become

$$\begin{aligned} \max_{\pi} V^{\pi}(s_0) \\ s_{t+1} = F(s_t, a_t) \\ s_0 \sim P_0(s) \end{aligned} \quad (13)$$

in practice.

Actor-Critic architecture is used in this paper. The value network (Critic), was trained by a V-trace method [4], which is a modified temporal difference (TD) learning [14]. The policy network (Actor), was trained according to (8) through hinge loss. In addition, since (8) can be satisfied by adjusting the likelihood per pair of state and action (s, a) , we replace the likelihoods by its log of likelihood for simplifying the

complexity in gradient calculation. The summarized objective is listed as follows

$$\begin{aligned} \min_{\theta_{\pi}} \max \{0, \xi - \hat{A}_t \log \frac{\pi(a_t|s_t)}{\mu(a_t|s_t)}\}, \\ \min_{\theta_v} \left| \hat{V}_t - V(s_t; \theta_v) \right|^2, \\ \hat{A}_t = r_t + \gamma V(s_{t+1}) - V(s_t) + \frac{\pi(a_{t+1}|s_{t+1})}{\mu(a_{t+1}|s_{t+1})} \hat{A}_{t+1}, \\ \hat{V}_t = V(s_t; \theta_v) + \frac{\pi(a_t|s_t)}{\mu(a_t|s_t)} \hat{A}_t, \\ \mathcal{T} = \{(s_i, a_i, s_{i+1}, \mu(a_i|s_i)) | i = 1 \dots T\} \in \mathcal{B}, \end{aligned} \quad (14)$$

where ξ is the margin to make the samples that already satisfied (8) not to provide losses for policy improvement [12].

Notice that since the simplified rigid body dynamic is independent to the rotor number. The different physical configurations are only effect on J and m , the trained RL policy could be implemented directly on to quadrotors. Unfortunately, training RL controller on simplified ideal environment and transfer to real world still exists system uncertainty and system response latency. These factors may lead to the quadrotor become unstable especially under aggressive maneuver situation. To overcome this problem, we consider a hybrid control strategy and introduce a tracking algorithm in next section.

III. SIMULATION ENVIRONMENT AND TRAJECTORY GENERATING RESULT

In this section, we used the aforementioned dynamic equations and reinforcement algorithms to train a quadrotor perching policy controlling the four motors output directly which can successfully landing on the vertical wall. The reward function for RL training is designed as follows

$$\text{reward} = - [w_1 e^{-d_x} \quad w_2 \quad w_3] [\| \mathbf{R}_e \| \quad \| \mathbf{x}_e \| \quad \| a \|]^T, \quad (15)$$

where \mathbf{R}_e , \mathbf{x}_e , and a are angle error, position error, and action output. w_1 to w_3 are the weights of the error, and d_x is the distance between quadrotor to the perching point on x -axis. For RL value and policy neural network construction, 3-layer with 32 and 128 nodes were used. The policy network outputs four motors thrust command to control the quadrotor perching task.

Once the quadrotor lands successfully in the simulator controlled by RL policy neural network, we extract the trained controller for generating feasible trajectory. The trajectory contains position, velocity, acceleration, jerk, and yaw angle information and use designed traditional controller to track along the planned path.

We design a sequence for controlling the quadrotor during operating the mission and can be separated into following three stages and shown in Fig.3:

- Stage I: Trajectories generation
- Stage II: Path following
- Stage III: Attitude control

In stage I, feasible trajectory would be generated from the current state of quadrotor and can successfully perch to desired point eventually. During the path following stage,

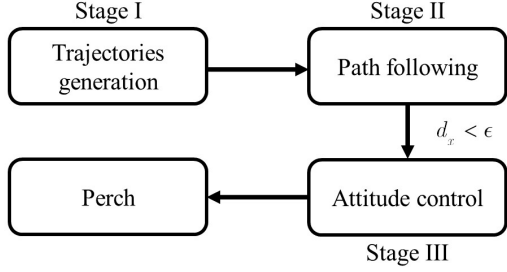


Fig. 3: Three stages of perching control sequence

the controller keeps tracking on the desired path with the information of position, velocity, acceleration, jerk, and yaw angle until the quadrotor approaches the launch point. As the distance d_x is shorter than designed threshold ϵ , quadrotor switch to stage III and attitude control would be triggered. During the attitude control stage, the controller attempt to stable the quadrotor to final pose and perch on the set point of a vertical plane. While the quadrotor reaching the original point with pitch angle of 90° , it would be considered to be a successful cases to landing onto the vertical surface.

IV. CONTROLLER DESIGN

In this section, we introduce our controller for trajectory tracking along perching neural network behavior. The tracking and perching consist of two controllers as follows,

1. Trajectory Tracking Control: controlling the quadrotor center of mass to follow the three-dimensional path including position, velocity, acceleration, and jerk information from RL trajectory generator.

2. Attitude Control: controlling the quadrotor to desired roll, pitch and yaw angle from trajectory tracking controller command.

A. Trajectory Tracking Control

The tracking controller is based on proportional-derivative (PD) controller and can be written as following expression,

$$\mathbf{a}_c = \mathbf{K}_x(\mathbf{x}_{ref} - \mathbf{x}_f) + \mathbf{K}_v(\mathbf{v}_{ref} - \mathbf{v}_f) + \mathbf{a}_{ref} \quad (16)$$

where \mathbf{a}_c is the desired acceleration vector of quadrotor, \mathbf{x}_{ref} , \mathbf{v}_{ref} , \mathbf{a}_{ref} are the control references from trajectory generator, \mathbf{x}_f , and \mathbf{v}_f are the feedback, and \mathbf{K}_x , \mathbf{K}_v are the gains of each component. The total thrust T_c and desired attitude expressed in rotation matrix form $(\mathbf{R}_c)_{Traj}$ can be derived as

$$\begin{aligned} T_c &= -m \|\mathbf{a}_c\| \cdot \mathbf{b}_z \\ (\mathbf{R}_c)_{Traj} &= [\mathbf{b}_{x_c} \ \mathbf{b}_{y_c} \ \mathbf{b}_{z_c}], \end{aligned} \quad (17)$$

where

$$\begin{aligned} \mathbf{e}_y &= [-\sin \psi_{ref}, \cos \psi_{ref}, 0]^T \\ \mathbf{b}_{z_c} &= \frac{\mathbf{a}_c}{\|\mathbf{a}_c\|} \\ \mathbf{b}_{x_c} &= \frac{\mathbf{e}_y \times \mathbf{b}_{z_c}}{\|\mathbf{e}_y \times \mathbf{b}_{z_c}\|} \\ \mathbf{b}_{y_c} &= \frac{\mathbf{b}_{z_c} \times \mathbf{b}_{x_c}}{\|\mathbf{b}_{z_c} \times \mathbf{b}_{x_c}\|} \end{aligned} \quad (18)$$

ψ_{ref} is the desired heading angle, and $\|\mathbf{e}_y \times \mathbf{b}_{z_c}\| > 0$ is always greater than 0 because the quadrotor would not operate upside down in trajectory tracking control.

B. Attitude Control

The attitude controller not only receive the $(\mathbf{R}_c)_{Traj}$ command from trajectory tracking control but also switch to final perching attitude $(\mathbf{R}_c)_P$. The controller consists of dual-loop control structure. The outer loop P control in (21) determines the desired angular velocity of quadrotor, where \mathbf{R}_c switches according to the distance of quadrotor to perching point on x -axis d_x .

$$\mathbf{R}_c = \begin{cases} (\mathbf{R}_c)_{Traj} & , d_x \geq \epsilon \\ (\mathbf{R}_c)_P & , 0 < d_x < \epsilon \end{cases} \quad (19)$$

The error of rotational angle between \mathbf{R}_c and measurement feedback \mathbf{R}_f is given by

$$\mathbf{e}_R = -0.5(\mathbf{R}_c^T \mathbf{R}_f - \mathbf{R}_f^T \mathbf{R}_c)^\vee \quad (20)$$

where the *vee map* \vee is the mapping $\text{SO}(3) \rightarrow \mathbb{R}^3$ [10], and the desired angular velocity Ω_c is derived as

$$\Omega_c = \mathbf{K}_R \mathbf{e}_R + \Omega_{ref}. \quad (21)$$

The Ω_{ref} is the feed-forward term given from trajectory tracking controller, which use the jerk of the trajectory to compensate angular velocity command of the quadrotor [15].

The inner loop uses a PID controller for desired angular acceleration shown in (22).

$$\begin{aligned} \mathbf{e}_\Omega &= -\Omega_f + \mathbf{R}_f^T \mathbf{R}_c \Omega_c \\ \dot{\Omega}_c &= \mathbf{K}_p \mathbf{e}_\Omega + \mathbf{K}_i \int \mathbf{e}_\Omega + \mathbf{K}_d \dot{\mathbf{e}}_\Omega \end{aligned} \quad (22)$$

where Ω_f is the feedback of quadrotor angular velocity.

The command of rotor speed is determined according to (9) (11) with T_c and $\dot{\Omega}_c$.

V. SIMULATION RESULTS

To verify that our proposed perching trajectory generating and tracking structure could successfully landing on the wall, we conduct 50 flight tests starting from arbitrary initial position and velocity in a $1\text{m} \times 1\text{m} \times 1\text{m}$ space in front of the perching point in the simulation environment illustrates in Fig. 2. All trails perch to the set position successfully. Fig. 4 shows four flight results start from different initial condition. Table. I shows the mean and standard deviation (SD) of the distance error and pitch angle while the The vehicles touch the wall. The simulation experiment shows while the quadrotor reach to $x = 0$, the mean distance error to the landing point on y and z is -0.47 cm and -1.74 cm. The mean pitch angle is -1.17° .

VI. CONCLUSION

In this paper, we present a quadrotor perching control structure which combining RL trajectory planning and traditional tracking controller. The complex nonlinear dynamic constrain optimization problem can be solved by using trained RL trajectory planner to find a feasible path rapidly. A well

TABLE I: Simulation results of sampling 50 trails and the mean contact position and SD on y, z -axis and pitch angle θ while the quadrotor reach position $x = 0$.

	Mean	SD
y -axis	-0.47 cm	0.2 cm
z -axis	-1.74 cm	0.21 cm
pitch angle	88.83°	0.62°

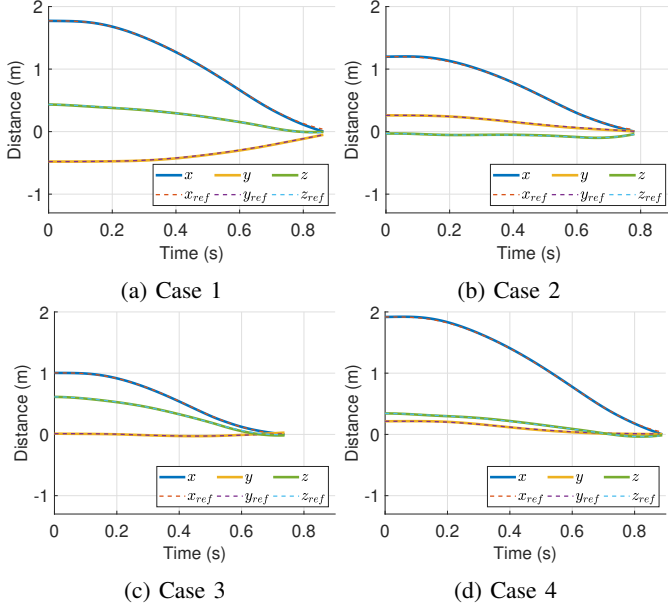


Fig. 4: Four cases of flight result start from different initial condition.

designed traditional controller can guarantee the stability of quadrotor. The control structure can make up the uncertainty using RL control policy output directly to motors when it has disturbance in operation or modeling imperfection in RL training process. The perching simulation in Section V demonstrates the quadrotor follows the trajectory generated by RL control policy and perches to designed point with standard deviation 0.2 cm on y, z -axis and pitch angle 88.83° in average on the wall.

Future work will focus on the real-world implementation, verify the overall control structure perching performance, and observing the robustness while facing disturbance and model uncertainties. However, the long term goal is to perform tasks physical contact such as battery charging or environment monitoring.

REFERENCES

- [1] Michele Bolognini and L. Fagiano. Lidar-based navigation of tethered drone formations in an unknown environment. *ArXiv*, abs/2003.12981, 2020.
- [2] K. Choutri, M. Lagha, and L. Dala. A fully autonomous search and rescue system using quadrotor uav. 2020.
- [3] P. Durdevic, D. Ortiz-Arroyo, and Z. Yang. Lidar assisted camera inspection of wind turbines: Experimental study. *2019 1st International Conference on Electrical, Control and Instrumentation Engineering (ICECIE)*, pages 1–7, 2019.
- [4] Lasse Espeholt, Hubert Soyer, R. Munos, K. Simonyan, V. Mnih, Tom Ward, Yotam Doron, Vlad Firoiu, T. Harley, Iain Dunning, S. Legg, and K. Kavukcuoglu. Impala: Scalable distributed deep-rl with importance weighted actor-learner architectures. *ArXiv*, abs/1802.01561, 2018.

- [5] L. Fagiano. Systems of tethered multicopters: Modeling and control design. *IFAC-PapersOnLine*, 50:4610–4615, 2017.
- [6] J. Hwangbo, I. Sa, R. Siegwart, and M. Hutter. Control of a quadrotor with reinforcement learning. *IEEE Robotics and Automation Letters*, 2:2096–2103, 2017.
- [7] A. Kalantari, Karan Mahajan, D. Ruffatto, and M. Spenko. Autonomous perching and take-off on vertical walls for a quadrotor micro air vehicle. *2015 IEEE International Conference on Robotics and Automation (ICRA)*, pages 4669–4674, 2015.
- [8] Evan Kaufman, Kuya Takami, Zhuming Ai, and Taeyoung Lee. Autonomous quadrotor 3d mapping and exploration using exact occupancy probabilities. *2018 Second IEEE International Conference on Robotic Computing (IRC)*, pages 49–55, 2018.
- [9] Taeyoung Lee. Geometric controls for a tethered quadrotor uav. *2015 54th IEEE Conference on Decision and Control (CDC)*, pages 2749–2754, 2015.
- [10] Taeyoung Lee, M. Leok, and N. McClamroch. Geometric tracking control of a quadrotor uav on se(3). *49th IEEE Conference on Decision and Control (CDC)*, pages 5420–5425, 2010.
- [11] Daniel Mellinger, Nathan Michael, and Vijay Kumar. Trajectory generation and control for precise aggressive maneuvers with quadrotors. *The International Journal of Robotics Research*, 31:664 – 674, 2012.
- [12] Chen-Huan Pi, Kai-Chun Hu, Stone Cheng, and I-Chen Wu. Low-level autonomous control and tracking of quadrotor using reinforcement learning. *Control Engineering Practice*, 95:104222, 2020.
- [13] Bjorn E. Schafer, D. Picchi, T. Engelhardt, and D. Abel. Multicopter unmanned aerial vehicle for automated inspection of wind turbines. *2016 24th Mediterranean Conference on Control and Automation (MED)*, pages 244–249, 2016.
- [14] R. Sutton. Learning to predict by the methods of temporal difference learning. 1988.
- [15] Ezra Tal and Sertac Karaman. Accurate tracking of aggressive quadrotor trajectories using incremental nonlinear dynamic inversion and differential flatness. *2018 IEEE Conference on Decision and Control (CDC)*, pages 4282–4288, 2018.
- [16] Justin Thomas. Grasping, perching, and visual servoing for micro aerial vehicles. 2017.
- [17] Justin Thomas, M. Pope, Giuseppe Loianno, E. Hawkes, M. A. Estrada, Hao Jiang, M. Cutkosky, and V. Kumar. Aggressive flight with quadrotors for perching on inclined surfaces. *Journal of Mechanisms and Robotics*, 8:051007, 2016.
- [18] Haijie Zhang, Jiefeng Sun, and Jianguo Zhao. Compliant bistable gripper for aerial perching and grasping. *2019 International Conference on Robotics and Automation (ICRA)*, pages 1248–1253, 2019.